AIP | Journal of Applied Physics

Surface effect on domain wall width in ferroelectrics

Eugene A. Eliseev, Anna N. Morozovska, Sergei V. Kalinin, Yulan Li, Jie Shen et al.

Citation: J. Appl. Phys. **106**, 084102 (2009); doi: 10.1063/1.3236644
View online: http://dx.doi.org/10.1063/1.3236644
View Table of Contents: http://jap.aip.org/resource/1/JAPIAU/v106/i8
Published by the American Institute of Physics.

Surface effect on domain wall width in ferroelectrics

Eugene A. Eliseev,[1,a)] Anna N. Morozovska,[1,b)] Sergei V. Kalinin,[2] Yulan Li,[3,c)] Jie Shen,[4] Maya D. Glinchuk,[1] Long-Qing Chen,[3] and Venkatraman Gopalan[3]
[1]*Institute for Problems of Materials Science, National Academy of Science of Ukraine, 3, Krjijanovskogo, Kiev 03142, Ukraine*
[2]*The Center for Nanophase Materials Sciences and Materials Science and Technology Division, Oak Ridge National Laboratory, Oak Ridge, Tennessee 37831, USA*
[3]*Department of Materials Science and Engineering, Pennsylvania State University, University Park, Pennsylvania 16802, USA*
[4]*Department of Mathematics, Purdue University, West Lafayette, Indiana 47907, USA*

(Received 19 July 2009; accepted 27 August 2009; published online 26 October 2009)

We study the effect of the depolarization field on a domain wall structure near the surface of a ferroelectric. Since in real situation bound and screening charges form an electric double layer, the breaking of this layer by the domain wall induces stray depolarization field, which in turn changes the domain wall structure. Power law decay of the stray field results in the power law of polarization saturation near the surface, as compared to exponential saturation in the bulk. Obtained results predict that the surface broadening of ferroelectric domain walls appeared near Curie temperature as well as describe domain wall depth profile in weak ferroelectrics. We qualitatively describe extra-broad domain walls near $LiNbO_3$ and $LiTaO_3$ surfaces observed experimentally at room temperature, which probably originate at high temperatures but did not fully relax their width with temperature decrease allowing for lattice pinning and defect centers. Thus results have broad implication for fundamental issues such as maximal information storage density in ferroelectric data storage, domain wall pinning mechanisms at surfaces and interfaces, and nucleation dynamics.
 [doi:10.1063/1.3236644]

I. INTRODUCTION

Surfaces, interfaces, and domain structures in spatially constrained ferroic materials have been attracting much attention since the early 1970s.[1–3] In the classical papers of Cao and Cross[4] and Zhirnov,[5] a single boundary between two domains in the bulk ferroelectrics was considered, allowing for the electrostriction effects. The stability of domain structure in the electroded thin films in the presence of dielectric dead layer was considered by Bratkovsky and Levanyuk,[6] while Pertsev and Kohlstedt[7] considered finite screening length in electrodes.

The domain wall thickness dependence on the slab thickness and other material parameter for ferroic stripe domains has been analyzed recently by Catalan *et al.*[8] They estimated the domain wall thickness and gradient coefficients in typical ferroelectric materials.

Despite the enormous progress achieved in atomistic and DFT modeling of multidomain ferroelectrics and domain wall behavior in thin films and its significant relevance to virtually all aspects of ferroelectric and other ferroic materials, the question of near-surface structure of a domain boundary in the proper ferroelectrics was virtually out of consideration; the only exception is the early work of Darinskii *et al.*[9] It was found that near the surface the ratio of the saturation value to the slope in the wall center is exactly the same as in the bulk. However, the domain wall profile near the surface was not analyzed. In contrast, in the paper we derive the domain wall profile near the surface self-consistently using perturbation theory.

II. EQUATIONS OF STATE

Spatial distribution of the polarization component P_3 inside the sample could be found from to the following equations of state:

$$(\alpha(T) - 2q_{ij33}u_{ij})P_3 + \beta_u P_3^3 + \delta P_3^5 - \zeta\frac{\partial^2 P_3}{\partial x_3^2} - \eta\left(\frac{\partial^2 P_3}{\partial x_2^2} + \frac{\partial^2 P_3}{\partial x_1^2}\right) = E_3^d, \quad (1)$$

$$-q_{ij33}P_3^2 + c_{ijkl}u_{lk} = \sigma_{ij}. \quad (2)$$

Coefficient $\alpha(T)=\alpha_T(T-T_C)$ explicitly depends on temperature T, gradient terms coefficients are $\zeta>0$ and $\eta>0$, expansion coefficients $\delta>0$, while $\beta_u<0$ for the first order phase transitions or $\beta_u>0$ for the second order ones. Here E_3^d is the depolarization field, caused by imperfect screening and inhomogeneous polarization distribution, u_{jk} are the strain tensor components, q_{ijkl} and c_{ijkl} are the components of electrostriction and elastic stiffness tensor correspondingly; σ_{ij} are the elastic stress tensor components. These equations should be supplemented by Maxwell equations for depolarization field, the conditions of mechanical equilibrium,[10,11] $\partial\sigma_{ij}/\partial x_i=0$, and compatibility relations for elastic field,

[a)]Electronic mail: eliseev@i.com.ua.
[b)]Electronic mail: morozo@i.com.ua. Permanent address: Institute of Semiconductor Physics, National Academy of Science of Ukraine, 41, pr. Nauki, 03028 Kiev, Ukraine.
[c)]Currently working in Pacific Northwest National Laboratory, Richland, WA 99354, USA.

$e_{ikl}e_{jmn}(\partial^2 u_{ln}/\partial x_k \partial x_m)=0$, where e_{ikl} is the permutation symbol or antisymmetric Levi–Civita tensor.

The boundary conditions for polarization could be obtained from the surface energy in the form[12]

$$\left(P_3 - \lambda_1 \frac{\partial P_3}{\partial x_3}\right)\Bigg|_{x_3=0} = 0, \qquad \left(P_3 + \lambda_2 \frac{\partial P_3}{\partial x_3}\right)\Bigg|_{x_3=L} = 0. \tag{3}$$

The introduced extrapolation length $\lambda_{1,2}$ may be different for $x_3=0$ and $x_3=L$, however, below we mainly consider the case of equal values $\lambda_{1,2}=\lambda$ for the sake of simplicity. Reported experimental values are $\lambda=2-50$ nm.[13,14]

The effect of *homogeneous* strain on ferroelectric properties could be simply incorporated by the renormalization of the expansion coefficient before P_3^4:

$$\beta = \beta_u - 4\frac{(q_{11}-q_{12})^2}{3(c_{11}-c_{12})} - 2\frac{(q_{11}+2q_{12})^2}{3(c_{11}+2c_{12})}. \tag{4}$$

For the case of *inhomogeneous* polarization distribution the strain field should satisfy the compatibility relation and consequently internal stress could appear. It was shown that inhomogeneous stress always exists in the vicinity of domain wall due to the electrostriction coupling.[4,5] The stress localization leads to the decrease in domain wall width in comparison with the case without electrostriction coupling:

$$R_\perp(T) = \sqrt{\frac{\eta}{\alpha(T) + (3\beta + 4q^2)P_S^2 + 5\delta P_S^4}},$$

$$q^2 \equiv \frac{2(q_{11}-q_{12})^2}{3(c_{11}-c_{12})} + \frac{(q_{11}+2q_{12})^2}{3(c_{11}+2c_{12})} - \frac{q_{12}^2}{c_{11}}. \tag{5}$$

Here $P_S(T)$ is the spontaneous polarization of mechanically free bulk system, determined from the equation $\alpha(T)+\beta P_S^2 + \delta P_S^4=0$.

Considering the elastic fields for fixed polarization distribution in the form of domain wall near the mechanically free flat surface we found that for the most of ferroelectrics the surface deviation from flatness and resulting changes of domain wall width near the surface are small (see Appendix D of supplementary materials[16]). So, in the case of the depolarization field absence, Eq. (5) could be reasonable approximation for domain wall halfwidth near the surface. Hereinafter we consider the impact of the imperfect screening on the near-surface domain structure and neglect the effect of elastic field changes near the mechanically free surface for sake of clarity.

III. DOMAIN WALL BROADENING CAUSED BY STRAY DEPOLARIZATION FIELDS

The depolarization field is determined by the spontaneous polarization inhomogeneity and/or its breaks at interfaces, as well as by the surrounding media. Below we consider ferroelectric short-circuited capacitor with dead layer between ferroelectric with inhomogeneous polarization distribution and electrode.

Hereinafter we consider uniaxial ferroelectrics with initial spontaneous polarization P_3^S directed along the polar axis

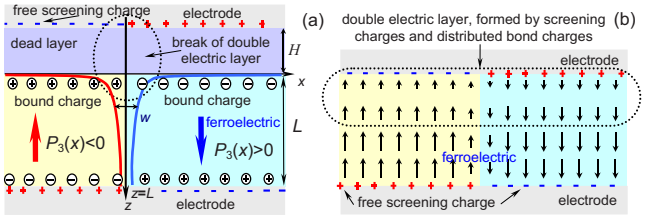

FIG. 1. (Color online) 180°-domain wall structure near the film surface. The double electric layer is formed due to either the physical dead layer (a) or intrinsic surface effect leading to diminished polarization at interface (b). Discontinuity of the double electric layer of screening and bound changes results in an additional stray depolarization field.

z. The sample is dielectrically isotropic in transverse directions, i.e., permittivity $\varepsilon_{11}=\varepsilon_{22}$ at zero external field. We assume that the dependence of in-plane polarization components on the inner field $E_{1,2}$ can be linearized as $P_{1,2} \approx \varepsilon_0(\varepsilon_{11}-1)E_{1,2}$. Thus the polarization vector acquires the form: $\mathbf{P}(\mathbf{r})=[\varepsilon_0(\varepsilon_{11}-1)E_1, \varepsilon_0(\varepsilon_{11}-1)E_2, P_3(\mathbf{E},\mathbf{r})]$. So, the Maxwell's equation div $\mathbf{D}=0$ for the displacement $\mathbf{D}=\mathbf{P}(\mathbf{r}) - \varepsilon_0 \nabla \varphi(\mathbf{r})$ expressed via electrostatic potential $\varphi(\mathbf{r})$, polarization $\mathbf{P}(\mathbf{r})$, and electric field $\mathbf{E}_{g,f}(x,y,z)=-\nabla\varphi_{g,f}(x,y,z)$. One can rewrite the Maxwell's equation for potential distribution as follows:

$$\frac{\partial^2 \varphi_g}{\partial z^2} + \frac{\partial^2 \varphi_g}{\partial y^2} + \frac{\partial^2 \varphi_g}{\partial x^2} = 0, \quad \text{for} \quad -H < z < 0, \tag{6a}$$

$$\varepsilon_0 \varepsilon_{33}^b \frac{\partial^2 \varphi_f}{\partial z^2} + \varepsilon_0 \varepsilon_{11}\left(\frac{\partial^2 \varphi_f}{\partial y^2} + \frac{\partial^2 \varphi_f}{\partial x^2}\right) = \frac{\partial P_3}{\partial z}, \quad \text{for} \quad 0 < z < L. \tag{6b}$$

Potentials φ_g and φ_f correspond to the dead layer with isotropic dielectric properties and ferroelectric film, respectively. Here the dielectric permittivity of the background or reference state[15] as ε_{33}^b (typically $\varepsilon_{33}^b \leq 10$); ε_0 is the dielectric constant of vacuum, L is the film thickness, H is the dead layer thickness (see Fig. 1). Equation (6) should be supplemented with the boundary conditions of zero top and bottom electrode potentials, continuous potential, and normal component of displacement on the boundaries between the dead layer and ferroelectric film. The isotropic dielectric permittivity of dead layer is ε_g. Fourier representation on transverse coordinates $\{x,y\}$ for electrostatic potential $\tilde{\varphi}(\mathbf{k},z)$ and electric field normal component $\tilde{E}_3=-\partial\tilde{\varphi}/\partial z$ inside the film ($0<z<L$) was derived in Appendix A of Ref. 16.

In order to estimate the depolarization field impact on the domain wall structure near the surface, let us consider the simple case of semi-infinite media ($L\to\infty$) with small difference of dielectric properties between ferroelectric and dead layer $\varepsilon_{33}^b \cong \gamma\varepsilon_g$, where the factor $\gamma=\sqrt{\varepsilon_{33}^b/\varepsilon_{11}}$. Assuming, that all uncompensated polarization bond charges are localized in thin near-surface layer [i.e., $\partial P_3(x,z>0)/\partial z \approx 0$], we derived that

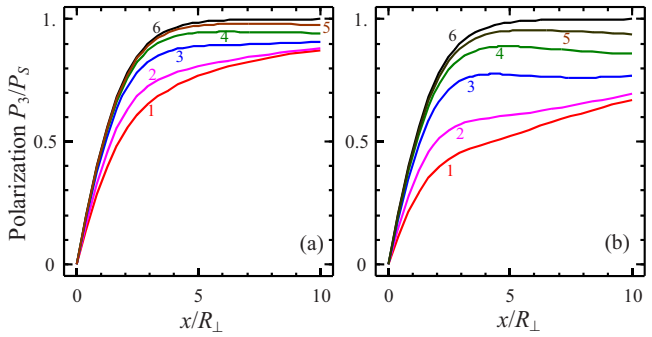

FIG. 2. (Color online) Normalized domain wall profile $P_3(x,z)/P_S$ calculated for different values of distances from the surface $z/R_\perp = 1,2,5,10,20,\infty$ (curves 1, 2, 3, 4, 5, 6) and dead layer thickness $H/R_\perp = 1,3$ [panels (a) and (b), respectively].

$$E_3(x,z) = -\int_{-\infty}^{\infty} d\tilde{x} \frac{P_3(x-\tilde{x})}{\pi\varepsilon_0(\varepsilon_{33}^b + \gamma\varepsilon_g)} \left(\frac{z/\gamma}{(z/\gamma)^2 + \tilde{x}^2} - \frac{z/\gamma + 2H}{(z/\gamma + 2H)^2 + \tilde{x}^2} \right). \quad (7)$$

Expression (7) has clear physical meaning: it is the sum on elementary linear charges placed at $z=0$ with density $d\tilde{x}P_3(x-\tilde{x})$, two terms in brackets correspond to electric field produced by the linear charge, and the field produced by its image correspondingly. In the case of abrupt domain wall, i.e., $P_3(x)=P_S\,\mathrm{sign}(x)$, Eq. (7) could be rewritten in the evident form as

$$E_3 = -\frac{(P_S/\varepsilon_0)}{\varepsilon_{33}^b + \gamma\,\varepsilon_g} \frac{2}{\pi} \left[\arctan\left(\frac{x}{z/\gamma} \right) - \arctan\left(\frac{x}{z/\gamma + 2H} \right) \right]. \quad (8)$$

Taking into account the self-consistent changes in depolarization field due to the induced polarization, the polarization distribution was derived as

$$P_3(x,z) \approx P_S(T) \left\{ \mathrm{sign}(x) - \frac{\varepsilon_{33}^f(T) - \varepsilon_{33}^b}{\varepsilon_{33}^f(T) + \gamma\varepsilon_g} \times \frac{4\pi x H}{(\pi|x| + 2z/\gamma)[\pi|x| + 2(z/\gamma + 2H)]} \right\}. \quad (9)$$

Here $\varepsilon_{33}^f(T) = \varepsilon_{33}^b + 1/[\varepsilon_0(\alpha(T) + 3\beta P_S^2 + 5\delta P_S^4)]$ is the full permittivity. It is seen from Eq. (9) that, even for abrupt initial domain wall, the emerging depolarization field induces polarization saturating as slow as $\sim 1/x$.

Since the factor of the order of $\sim P_S/(\varepsilon_0\varepsilon_{33}^f)$ is much higher than thermodynamic coercive field, the stray field (8) would influence the polarization distribution at distances z much higher than dead layer thickness H. Actually, it is clear from the Fig. 2 that in the range $z \gg H$ one could hardly say about the length H as the scale of polarization (9) and depolarization field (8), but H determines the amplitude. In the next section we consider the results of more rigorous consideration of this effect, allowing for the intrinsic width of domain wall, polarization gradient contribution, and the influence of the finite thickness of ferroelectric film.

IV. DOMAIN WALL BROADENING CAUSED BY THE SURFACE INFLUENCE AT TEMPERATURES NEAR CURIE POINT

As it was discussed in Sec. II, one could neglect the changes in spontaneous strain distribution caused by the stress realization near the free surface and use Eq. (1) after the substitution of strain field, obtained by Cao and Cross.[4] Using designations (4) and (5), the resulting equation for polarization distribution has the view:

$$(\alpha - 2q^2P_S^2)P_3 + (\beta + 2q^2)P_3^3 + \delta P_3^5 - \zeta\frac{\partial^2 P_3}{\partial z^2} - \eta\left(\frac{\partial^2 P_3}{\partial x^2} + \frac{\partial^2 P_3}{\partial y^2} \right) = E_3^d. \quad (10)$$

Note that, despite electrostriction renormalization in Eq. (10), the spontaneous polarization value far from the wall and surfaces is not affected in contrast to the renormalization of domain wall bulk width given by Eq. (5). The fact allows us to consider the influence of stray depolarization field on the domain wall structure in uniaxial proper ferroelectrics using perturbation theory. The polarization profile across the domain wall is represented as

$$P_3(x,z) = P_0(x) + p(x,z). \quad (11)$$

Function $P_0(x)$ is the polarization profile unperturbed by the surface influence or "bulk" one-dimensional (1D) domain structure. Perturbation of bulk domain structure $p(x,z)$ is caused by the stray depolarization field. In order to simplify further consideration, we ignore the dead layer, putting $H=0$. In this case the only source of depolarization field is the changes in polarization due to the surface influence.

For the first order ferroelectrics the single domain wall bulk profile corresponds to 1D solution of Eq. (10) in the absence of depolarization field (see, e.g., Ref. 4):

$$P_0(x) = \frac{P_S(T)\sinh[(x-x_0)/2R_\perp]}{\sqrt{\cosh^2[(x-x_0)/2R_\perp(T)] + 2\delta P_S^2(3\beta + 6q^2 + 4\delta P_S^2)}}. \quad (12)$$

Equation (12) reduces to $P_0(x)=P_S(T)\tanh[(x-x_0)/2R_\perp]$ for the second order ferroelectrics. Correlation radius $R_\perp(T)$ is given by Eq. (5), the position of the domain wall center is $x=x_0$.

In order to find the perturbation of bulk domain structure, $p(x,z)$, we linearized Eq. (10) allowing for substitution (11). For the second order ferroelectrics direct integration for semi-infinite sample leads to the approximate analytical expression (see Appendix B of Ref. 16 for details):

$$P_3(x,z) \approx \left(1 - \frac{\exp(-z/\sqrt{\varepsilon_{33}^b\varepsilon_0\zeta})}{1 + \lambda/\sqrt{\varepsilon_{33}^b\varepsilon_0\zeta}} \right) P_S \tanh\left(\frac{x-x_0}{2R_\perp} \right) - \frac{d}{4R_\perp}\sqrt{\frac{\varepsilon_{11}}{\varepsilon_{33}^f}} \times \ln\left(\frac{(2R_\perp + x - x_0)^2 + (\varepsilon_{11}/\varepsilon_{33}^f)(z+d)^2}{(2R_\perp - x + x_0)^2 + (\varepsilon_{11}/\varepsilon_{33}^f)(z+d)^2} \right) P_S, \quad (13)$$

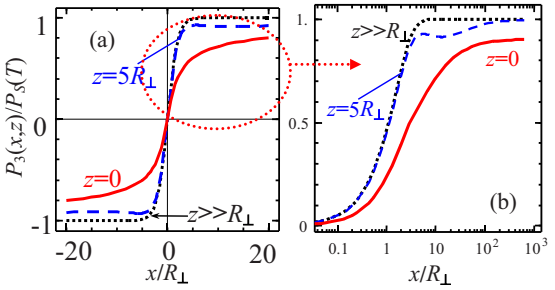

FIG. 3. (Color online) Normalized domain wall profile $P_3(x,z)/P_S(T)$ calculated at fixed temperature T for $R_z=R_\perp$ and extrapolation length $\lambda=0.5R_\perp$. (a) Profile in linear scale and (b) half-profile in log-linear scale. Solid, dashed, and dotted curves correspond to different distances $z/R_\perp=0,5,\infty$ from the surface of thick film ($L\gg R_z$).

where the distance $d=\zeta/\{[\alpha+(3\beta+4q^2)P_S^2](\sqrt{\varepsilon_{33}^b\varepsilon_0\zeta}+\lambda)\}$. It is clear from Eq. (13) that finite extrapolation length effect provides power law saturation of domain wall profile (the last logarithmic term should be expanded far from the wall), which is much slower compared to exponential saturation of bulk profile $P_0(x)$. At distances $|x-x_0|\gg R_\perp(T)$ the latter term behaves as $2(x-x_0)/[(x-x_0)^2+(\varepsilon_{11}/\varepsilon_{33}^f)(z+d)^2]$, which is the distribution of stray depolarization field far from the break of double electric layer. The quantity d plays the role of effective double layer (screening layer) width. Expression (13) explains power saturation of domain wall profiles as the direct effect of the depolarization field that decreases much slowly in comparison with exponential saturation of bulk profile "$\tanh[(x-x_0)/2R_\perp]$" [see Figs. 3(a) and 3(b)].

In Fig. 3 we presented results of calculations at fixed temperature below critical value (and normalized coordinate and extrapolation length on the only relevant parameter, correlation radius). At the same time, due to the complicated temperature dependence of Eqs. (12) and (13), we expect that approaching the phase transition could reveal some interesting features of the obtained results (see Fig. 4). Note, that here we normalized temperature-independent coordinate and extrapolation length on the correlation radius at zero temperature.

It is evident from Fig. 4 that the higher the correlation radius $R_\perp(T)$ (e.g., T is close to Curie temperature T_C), the strongest is the domain wall broadening. When approaching the transition temperature both the bulk wall width and the effect of interface on the width increase. However the increase in interface influence region [see Fig. 4(d)] is more pronounced than those of bulk width, since the latter scales with temperature as $(-\alpha)^{-1/2}$ while the former governed by the double layer effective width d scales as $(-\alpha)^{-1}$. Qualitatively the same effect of finite extrapolation length and inhomogeneous elastic stress on periodic 180°-domain structure near the film surface was obtained numerically by using phase field method (see Fig. 5 here and Appendix E of Ref. 16).

Calculated width of domain wall w at level 0.76 as a function of depth z from the sample surface is shown in Figs. 6(a) and 6(b) for $PbZr_{0.5}Ti_{0.5}O_3$ material parameters and equal extrapolation lengths λ for both film surfaces. It is evident that smaller extrapolation length leads to the strongest broadening [compare plots (a) and (b)].

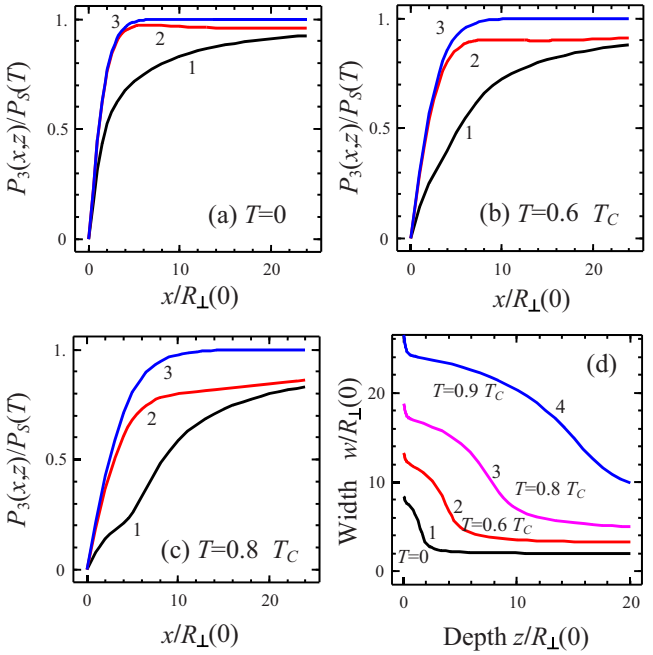

FIG. 4. (Color online) Domain wall profiles at different temperatures $T/T_C=0,0.6,0.8$ [panels (a)–(c), respectively]. Curves 1–3 correspond to different distances $z/R_\perp(T=0)=1,10,\infty$ from the surface of thick film ($L\gg R_z$). (d) Domain wall half width $w(z)/R_\perp(T=0)$ (at level 0.76) as the function of depth z at different temperature values, specified near the curves. $R_z=R_\perp$, extrapolation length $\lambda=2R_\perp(T=0)$.

Calculated width (solid curves) of domain wall at level 0.76 as a function of its depth from the surface of $LiTaO_3$ is shown in Fig. 6(c) in comparison with experimental data[17,18] in 500 nm thick stoichiometric $LiTaO_3$ (squares) and 50 nm thick congruent $LiTaO_3$ (triangles). Experimental data are taken as is, without analysis of possible finite resolution effects. However, recent observations of atomically resolved scanning nonlinear dielectric microscopy (SNDM) image

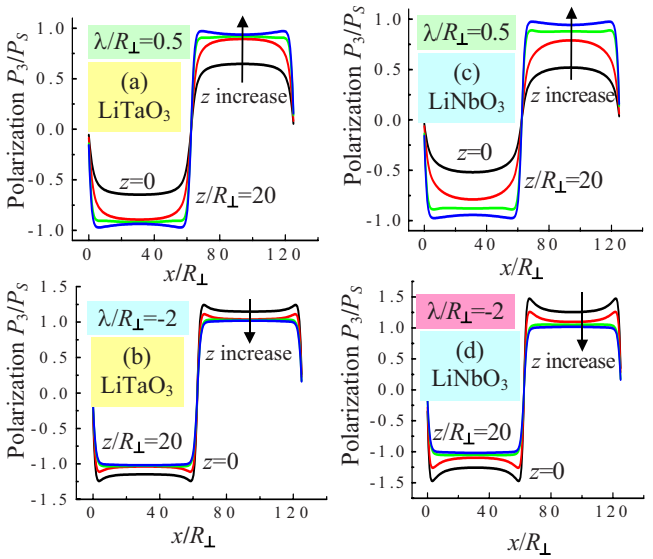

FIG. 5. (Color online) Domain structure near the surface of $LiTaO_3$ (a), (b) and $LiNbO_3$ (c), (d) films calculated numerically by using phase field method for $R_z=R_\perp$ [(a) and (b)] and $R_z=1.5R_\perp$ [(c) and (d)], extrapolation length $\lambda=0.5R_\perp$ [(a) and (c)] $\lambda=-2R_\perp$ [(b) and (d)] and different distances from the surface $z=0$, $0.5R_\perp$, $5R_\perp$, and $20R_\perp$.

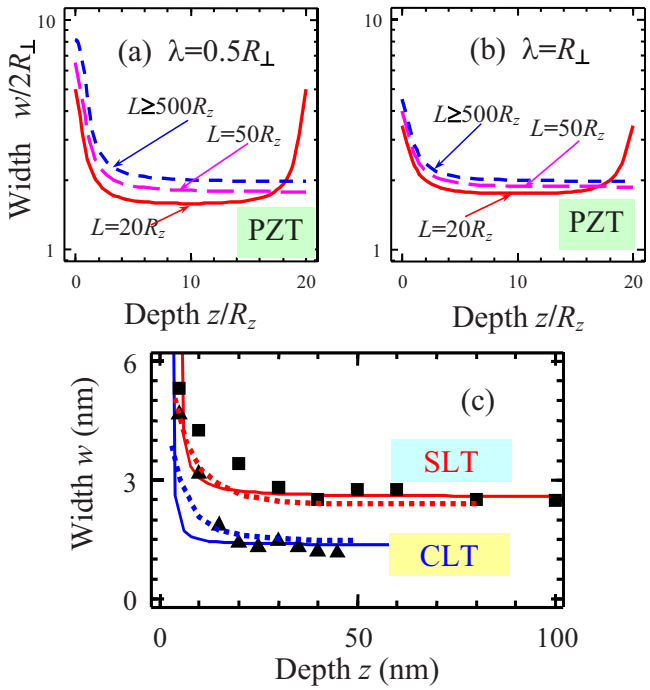

FIG. 6. (Color online) [(a) and (b)] Thickness of domain wall $w/2R_\perp$ at level 0.76 as a function of depth z from the surface at $R_z=R_\perp$, extrapolation length $\lambda=0.5R_\perp$ (a), and $\lambda=R_\perp$ (b) for material parameters of $PbZr_{0.5}Ti_{0.5}O_3$. (c) Thickness of domain wall at level 0.76 as a function of its depth from the surface of $LiTaO_3$. Squares are experimental data from Refs. 17 and 18 for 500 nm thick stoichiometric $LiTaO_3$ (SLT), and triangles correspond to 50 nm thick congruent $LiTaO_3$ (CLT). Solid curves are analytical calculations for fitting parameters $R_\perp=1.3$ nm, $R_z=1.6$ nm, different extrapolation lengths $\lambda_1(0)=0.1$ nm, and ($\lambda_2(h)$ value appeared not important), for SLT; while $R_\perp=0.7$ nm, $R_z=1.4$ nm and $\lambda_1(0)=0.1$ nm, $\lambda_2(h) \gg 30$ nm for CLT. Corresponding dotted curves are numerical calculations by phase field modeling for the same fitting parameters.

suggest that resolution can be higher or comparable with measured wall width.[19] When calculating the curve for 50 nm thick $LiTaO_3$ film we take into account that domain wall profile w is strongly asymmetric, namely, at the surface $z=0$ the width is five times bigger than saturated "bulk" value near the surface $z=L$. Therefore we conclude that extrapolation length $\lambda_2(L) \gg \lambda_1(0)$. For the case $\lambda_2 \to \infty$ domain wall broadening is essential only near the surface $z=0$ (where λ_1 is finite), while the surface $z=L$ is indistinguishable from the bulk. Thus for $\lambda_2 \to \infty$, one should use expression (19) for profile calculations inside the film ($0 \le z \le L$) after the substitution of double thickness $2L$.[20] Dotted curves in Fig. 6(c) are numerical calculations by using phase field method.[21] It is clear from Fig. 6(c) that analytical calculations are in a reasonable agreement with experimental data and numerical simulations. The presence of damaged surface layer, reported in Refs. 17 and 18, and unmeasured surface polarization value allow us to consider finite extrapolation length value as a fitting parameter.

Considering the alternative explanation of the domain walls widening near the surface in $LiTaO_3$ due to their interaction with defects having larger density near the surface, we should note the following. Daimon and Cho[17,18] fabricated and examined two types of $LiTaO_3$ films: congruent (with numerous defects) and stoichiometric (almost without defects). Results for both types of samples demonstrated domain walls surface broadening, proving that the effect is defect independent.

V. CONCLUSION

The polarization behavior and domain wall broadening on the ferroelectric wall-surface junction is analyzed. We demonstrate that even when an electrode or ambient screening minimizes depolarization field, stray depolarization field leads to the changes in domain wall structure near the surface. Notably, the wall profile follows a long-range power-law profile at the surface, as opposed to an exponential saturation of the order parameter in the bulk. The saturation law is explained by the behavior of stray depolarization field that decreases like the field created by the break of double electric layer.

Obtained results predict the surface broadening of ferroelectric domain walls at temperatures near Curie point as well describe domain wall depth profile in weak ferroelectrics like Rochelle salt. Also we qualitatively describe extra-broad domain walls near $LiNbO_3$ and $LiTaO_3$ surfaces observed at room temperature, which probably originate at high temperatures but did not fully relax their width with temperature decrease allowing for lattice pinning and defect centers.

ACKNOWLEDGMENTS

Research was partially (E.A.E. and M.D.G.) supported by the Science and Technology Center in Ukraine, Project No. 3306. The research is supported in part (S.V.K.) by the Division of Scientific User Facilities, DOE BES. V.G. wishes to gratefully acknowledge financial support from the National Science Foundation Grant Nos. DMR-0602986, 0512165, 0507146, and 0213623, and CNMS at Oak Ridge National Laboratory. L.Q. and Y.L. are supported by DOE under Grant No. DE-FG02-07ER46417 and Los Alamos National Laboratory. Research also sponsored by Ministry of Science and Education of Ukrainian (Grant No. UU30/004) and National Science Foundation (Materials World Network, DMR-0908718).

[1] R. Kretschmer and K. Binder, Phys. Rev. B **20**, 1065 (1979).
[2] E. V. Chensky and V. V. Tarasenko, Zh. Eksp. Teor. Fiz. **83**, 1089 (1982) [Sov. Phys. JETP **56**, 618 (1982)].
[3] J. Junquera and Ph. Ghosez, Nature (London) **422**, 506 (2003).
[4] W. Cao and L. E. Cross, Phys. Rev. B **44**, 5 (1991).
[5] V. A. Zhirnov, Zh. Eksp. Teor. Fiz. **35**, 1175 (1959) [Sov. Phys. JETP **8**, 822 (1959)].
[6] A. M. Bratkovsky and A. P. Levanyuk, Phys. Rev. Lett. **84**, 3177 (2000).
[7] N. A. Pertsev and H. Kohlstedt, Phys. Rev. Lett. **98**, 257603 (2007).
[8] G. Catalan, J. F. Scott, A. Schilling, and J. M. Gregg, J. Phys.: Condens. Matter **19**, 022201 (2007).
[9] B. M. Darinskii, A. P. Lazarev, and A. S. Sidorkin, Fiz. Tverd. Tela (Leningrad) **31**, 287 (1989) [Sov. Phys. Solid State **31**, 2003 (1989)].
[10] S. P. Timoshenko and J. N. Goodier, *Theory of Elasticity* (McGraw-Hill, New York, 1970).
[11] L. D. Landau and E. M. Lifshitz, *Theory of Elasticity: Theoretical Physics* (Butterworth-Heinemann, Oxford, 1976), Vol. 7.
[12] M. D. Glinchuk, E. A. Eliseev, V. A. Stephanovich, and R. Farhi, J. Appl. Phys. **93**, 1150 (2003).
[13] C.-L. Jia, V. Nagarajan, J.-Q. He, L. Houben, T. Zhao, R. Ramesh, K. Urban, and R. Waser, Nature Mater. **6**, 64 (2007).
[14] M. D. Glinchuk, E. A. Eliseev, A. Deineka, L. Jastrabik, G. Suchaneck, T.

Sandner, G. Gerlach, and M. Hrabovsky, Integr. Ferroelectr. **38**, 101 (2001).
[15]C. H. Woo and Y. Zheng, Appl. Phys. A: Mater. Sci. Process. **91**, 59 (2008).
[16]See EPAPS supplementary material at http://dx.doi.org/10.1063/1.3236644 for the details of electric, elastic fields, and polarization distribution calculation.
[17]Y. Daimon and Y. Cho, Jpn. J. Appl. Phys., Part 2 **45**, L1304 (2006).
[18]Y. Daimon and Y. Cho, Appl. Phys. Lett. **90**, 192906 (2007).
[19]Y. Cho and R. Hirose, Phys. Rev. Lett. **99**, 186101 (2007).
[20]The result is evident from the symmetry considerations.
[21]Y. L. Li, S. Y. Hu, Z. K. Liu, and L.-Q. Chen, Acta Mater. **50**, 395 (2002).